Available online at www.sciencedirect.com
ScienceDirect
Journal of Luminescence 128 (2008) 199–204
JOURNAL OF LUMINESCENCE
www.elsevier.com/locate/jlumin

Improved electroluminescence performance of ZnS:Cu,Cl phosphors by ultrasonic treatment

Wendeng Wang, Fuqiang Huang*, Yujuan Xia, Anbao Wang

State Key Laboratory of High Performance Ceramics and Superfine Microstructure, Shanghai Institute of Ceramics, Chinese Academy of Sciences, Shanghai 200050, PR China

Received 9 February 2007; received in revised form 28 May 2007; accepted 5 July 2007
Available online 20 August 2007

Abstract

ZnS:Cu,Cl electroluminescence (EL) phosphors were prepared by high-temperature (1150 °C) solid-state reaction, subsequent ultrasonic treatment ($t = 0$–60 min) and final low-temperature annealing process at 750 °C. The as-synthesized phosphors were characterized by X-ray powder diffraction (XRD), UV–vis absorbance spectra, electron probe microanalyzer (EPMA) and photoluminescence (PL) spectra. EL performance was investigated on an EL lamp fabricated by screen-printing at 100 V and 400 Hz. Ultrasound irradiation leads to intensity reductions and width increases of some XRD diffraction peaks, and results in a slight red-shift of UV–vis absorption edge. It also exhibits strong influences on PL and EL properties of the phosphors. Generally, PL performance monotonically declines with the increase of ultrasonic time, while EL performance benefits from the ultrasonic treatment and is superior to that of the commercial ones. The defects in the microstructure induced by the ultrasonic treatment are the fundamental reason for the change of PL and EL performances.
© 2007 Elsevier B.V. All rights reserved.

PACS: 78.60.Fi; 43.35.+d

Keywords: Electroluminescence; Phosphors; ZnS; Ultrasonic

1. Introduction

Electroluminescent phosphors have commercial values in light emitting diodes (LEDs) and flat panel displays (FPDs) [1,2]. Powder electroluminescence (EL) devices are employed to liquid crystal display (LCD) backlight such as cell phones, personal digital assistant (PDA) and palmtop computer [3]. Up to now, one of the most important inorganic electroluminescent phosphors is ZnS-type materials activated by transition or rare-earth metals [4–6]. Among them, copper-activated ZnS phosphors with green–blue emission have attracted great attention and are extensively researched [4,5,7–9]. The usual synthesis route for ZnS:Cu EL powders is the conventional solid-state reaction. In this process, ZnS particles were mixed with activator salts and flux. Then the copper activator cations diffuse into ZnS particle matrix during the subsequent annealing treatment [10,11]. Recently, new methods have also been developed for the fabrication of ZnS-based phosphors [12–15]. Ultrasonic wave is widely utilized in many areas, for example, to synthesize nanomaterials [16]. However, the effect of ultrasonic treatment on the properties of ZnS:Cu phosphor is rarely studied. Motivated by the fact, in this study, we synthesized ZnS:Cu,Cl phosphors by two heat treatments with an intermediate ultrasonic treatment. The results show that photoluminescence (PL) performance of the as-prepared phosphors monotonically declines with the increase of ultrasonic time while EL performance benefits from ultrasonic treatment and is superior to that of the commercial ones.

*Corresponding author. Tel.: +86 21 52411620; fax: +86 21 52413903.
E-mail address: huangfq@mail.sic.ac.cn (F. Huang).

0022-2313/$ - see front matter © 2007 Elsevier B.V. All rights reserved.
doi:10.1016/j.jlumin.2007.07.003

2. Experimental

2.1. Preparation of the ZnS:Cu,Cl phosphors

All the reagents purchased from Sinopharm Chemical Reagent Co. (Shanghai, China) were of high purity (>99.99%). The ZnS:Cu,Cl phosphors were synthesized via the following three steps:

(a) *First firing*: ZnS, 0.236 wt% $CuSO_4 \cdot 5H_2O$ (600 ppm Cu), 3 wt% S, 2 wt% NaCl and 3 wt% $MgCl_2 \cdot 2H_2O$ were dryly ball-milled and calcined in a well-covered alumina crucible at 1150 °C for 3 h in air. The fired powders were then washed with hot deionized water to remove the flux, filtered and dried.
(b) *Ultrasonic treatment*: The slurry of 50 g obtained powders in 400 mL deionized water was mechanically stirred in a beaker, as shown in Fig. 1. The slurry was subjected to ultrasonic irradiation (Sonics & Materials, Inc., model VCX 750, frequency 20 kHz) for a specified time (0–60 min) and amplitude (power output 650 W). The temperature of the slurry was set below 50 °C to prevent water evaporation.
(c) *Second firing*: The ultrasonicated powders were dried at 120 °C and annealed in well-covered alumina crucibles at 750 °C for 2 h in air. The resulting powders were washed with water, dilute acetic acid (3 mol/L) and then with KCN solution. The obtained powders were washed again with deionized water to remove KCN and dried at 120 °C.

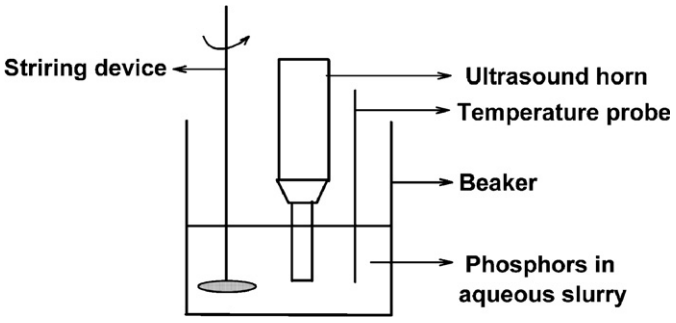

Fig. 1. The setup used to ultrasonicate the phosphors.

2.2. Characterization of the as-prepared phosphors

X-ray powder diffraction (XRD) patterns were determined on a Rigaku D/max-2550 V diffractometer using Cu K_α radiation ($\lambda = 0.15418$ nm). Scanning electronic images were obtained on a JEOL JXA-8100 electron probe microanalyzer (EPMA). The particle size was measured by Malvern particle size analyzer. UV–vis absorbance spectra were investigated at room temperature on a HITACHI U-3010 spectrophotometer. PL spectra were obtained on a Shimadzu RF-5301PC spectrofluorophotometer with a Xe lamp as the excitation source at room temperature. EL performance was investigated on an EL lamp at 100 V and 400 Hz. The EL lamp was fabricated by screen-printing, as shown in Fig. 2. It was composed of moisture-resistant film, PET (polyethylene terephthalate) substrate coated with ITO (indium tin oxide), copper conductive wire, phosphor layer, $BaTiO_3$ dielectric layer, silver conductive layer and moisture-resistant film. The phosphor, $BaTiO_3$ and silver layers were screen-printed by using the slurries of the related powders, binder and solvent, respectively.

3. Results and discussion

3.1. EPMA, particle size and XRD analysis

Fig. 3 presents the scanning electron image of the phosphor treated by ultrasonic irradiation for 60 min and then annealed at 750 °C. It can be seen that the particle size is relatively uniform and the mean size is about 21.2 μm.

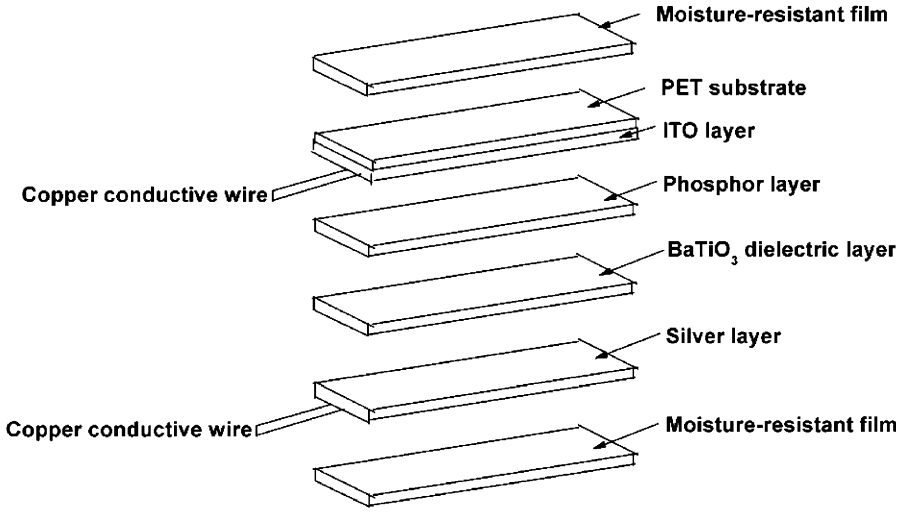

Fig. 2. The construction of the EL lamp.

This is in accord with the results obtained by the Malvern particle size analyzer, from which the 10%, 50% and 90% average particle sizes of the powders are determined to be 16.14, 22.08 and 32.47 μm, respectively.

Fig. 4a and b shows XRD patterns of the samples ultrasonicated for 0–60 min before and after the annealing process at 750 °C, respectively. We can see that the first firing at 1150 °C produced almost 100% hexagonal phase because bulk ZnS transforms from cubic to hexagonal phase at about 1020 °C [17]. However, in order to obtain efficient EL performance, it was necessary to change a part of hexagonal phase to cubic phase [13,18,19]. This was successfully realized by the ultrasonic treatment. It should be noted that during the ultrasonication, the acoustic energy of the transducer is concentrated in a small volume and only a portion of the suspension is being irradiated at a particular time. Computer simulation results on the phase ratios of the powders obtained after the annealing at 750 °C are included in Fig. 4b [20], showing that the cubic phase increases with a longer ultrasonic time. This was also confirmed by the fact that the diffraction peak of [1 0 1] plane attributed to the hexagonal phase becomes lower. Hence, ultrasonic treatment is beneficial to convert the hexagonal phase to cubic phase and the increase of ultrasonic time favors the formation of more cubic phase in the phosphors. The diffraction peaks of unannealed samples become broader with the increase of ultrasonic time (see Fig. 4c), accompanied with greater background noise near the peaks. It suggests that the ultrasonic treatment induces a distorted hexagonal or cubic crystalline form of ZnS from its high-temperature hexagonal crystallographic form, associated with non-uniform strain or residual stress. As shown in Fig. 4b, the diffraction peaks of the samples after the annealing treatment become smoother, revealing that the strain or stress induced by the ultrasonic irradiation was partly eliminated.

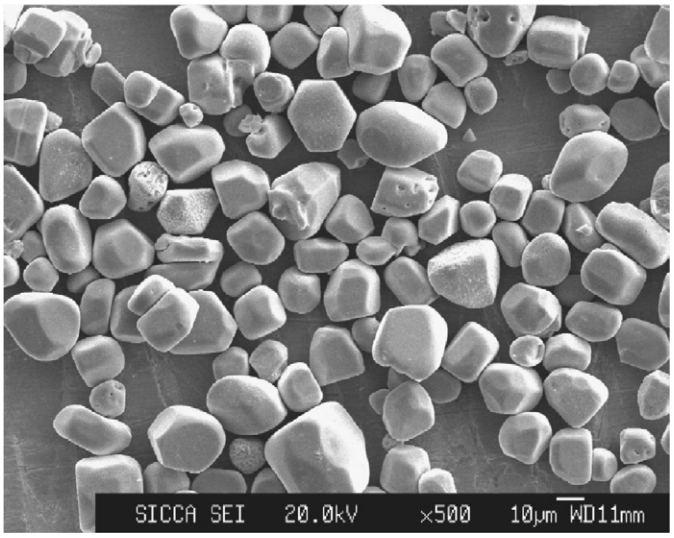

Fig. 3. Scanning electronic image of the phosphor treated by 60 min ultrasonic irradiation and then annealed at 750 °C.

3.2. UV–vis absorbance spectra

Fig. 5 illustrates the UV–vis absorbance spectra of the phosphors ultrasonicated for 0–60 min after the annealing treatment. The inset is the variation of band gap (E_g) of the samples with ultrasonic time. The absorption edge wavelength (λ_g) was determined from the intersection of the base line with the tangent drawn to the band shoulder, and the band gap was calculated by the equation

$$E_g(\text{eV}) = \frac{1240}{\lambda_g(\text{nm})}. \quad (1)$$

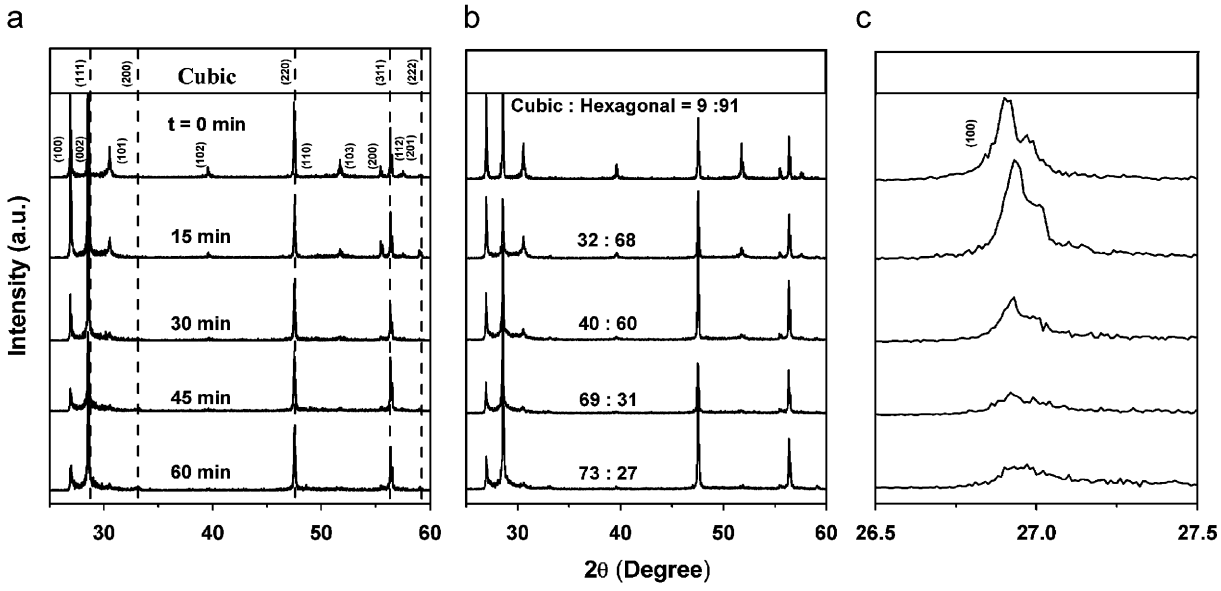

Fig. 4. XRD patterns of the samples ultrasonicated for 0–60 min before (a) and after (b) the annealing process at 750 °C. Figure in (c) is the enlarged view of (a) in the range of 26.5–27.5°.

The increase of ultrasonic time led to a slight red-shift of the absorption edge. After ultrasonic treatment of 60 min, the absorption edge of the sample has a red-shift of about 5.4 nm (389.2 → 394.6 nm), corresponding to the change of about 0.056 eV in the optical band gap (3.189 → 3.145 eV). This may be due to that the crystalline particles in the samples with a longer ultrasonic time possess more cubic phase as mentioned above. On the other hand, a longer ultrasonic irradiation time may induce more defects. This is another possible reason responsible for the red-shift.

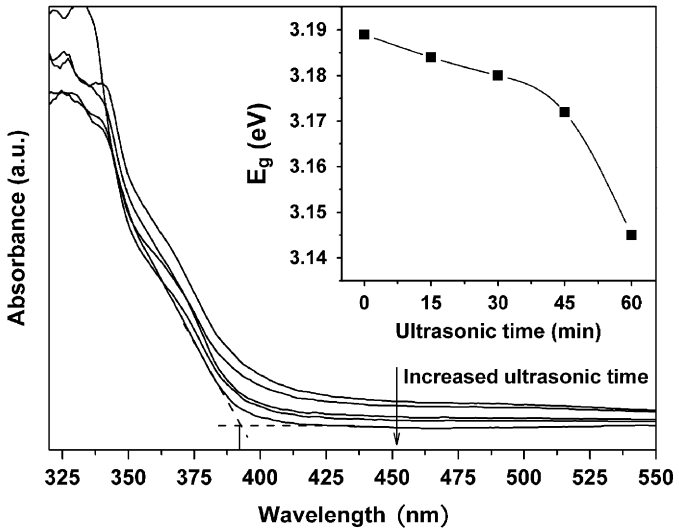

Fig. 5. UV–vis absorbance spectra of the phosphors ultrasonicated for 0–60 min after the annealing process. The inset is the band gap (E_g) of the samples vs. ultrasonic time.

3.3. PL properties

Fig. 6a and b, respectively, displays the PL excitation and emission spectra of the phosphors after the second firing at 750 °C. Both the optimal excitation wavelength (331–335 nm) and emission peaks (509–515 nm) remain almost unchanged while the intensity of the excitation and emission bands monotonically reduce with the ultrasonic time increasing. Therefore, the influence of the ultrasonic treatment on PL intensity is obvious. As shown in the inset of Fig. 6b, the emission intensity of the phosphor decreased as much as 51% (102.3 → 50.3) after the ultrasonic treatment of 60 min. As discussed above, a longer ultrasonic irradiation time may induce more defects, causing the increase of trapping or non-radiative recombination centers. This is the main reason that the PL performance is deteriorated with the increase of ultrasonic time.

3.4. EL properties

Table 1 summarizes the EL performance comparisons between the phosphors prepared in this work and the commercial ones (Nemoto Co. Ltd., Japan; average particle size 22 μm), including 2 h brightness (I2), 24 h brightness

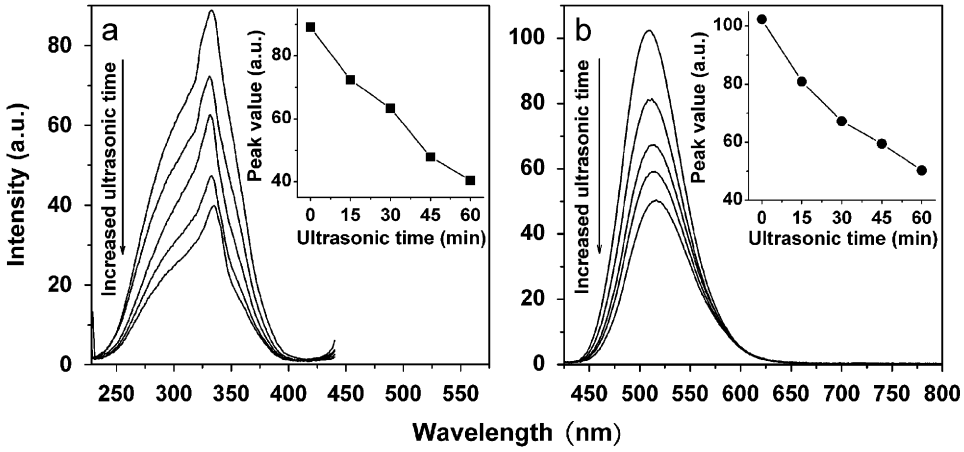

Fig. 6. The PL excitation spectra (a) and emission spectra (b) of the phosphors after the annealing process at 750 °C.

Table 1
EL performance comparisons between the phosphors prepared in this work and the commercial ones (Nemoto Co. Ltd., Japan; average particle size 22 μm)

Ultrasonic time (min)	2 h brightness (cd/m^2)	24 h brightness (cd/m^2)	Color coordinates (x, y)	Efficacy (lm/W)	Maintenance (I24/I2)
0	42.09	36.32	(0.184, 0.416)	4.75	0.85
15	114.59	103.13	(0.185, 0.432)	5.97	0.90
30	125.48	113.06	(0.187, 0.445)	5.68	0.91
45	118.50	109.97	(0.188, 0.458)	4.01	0.93
60	109.92	99.72	(0.188, 0.460)	4.67	0.92
Commercial	106.26	95.85	(0.183, 0.468)	5.62	0.90

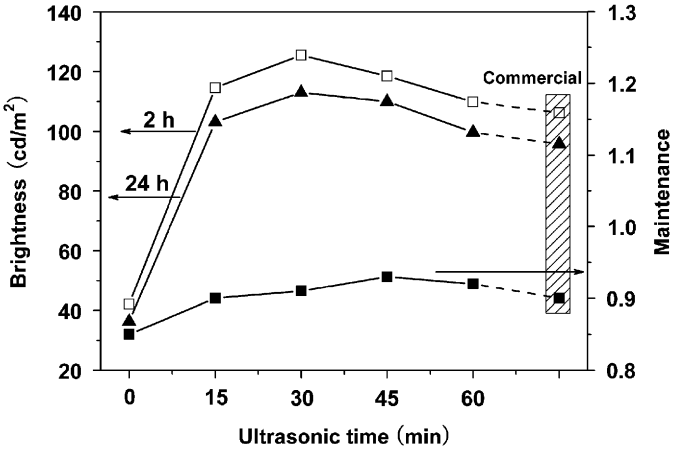

Fig. 7. The dependence of 2 h, 24 h brightness (I2, I24) and maintenance (I24/I2) on the ultrasonic time.

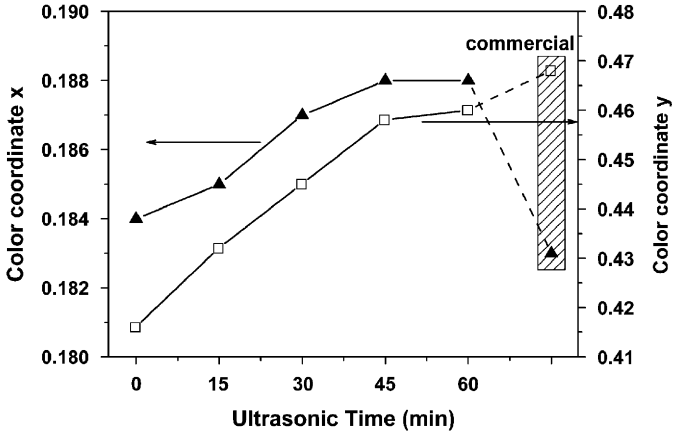

Fig. 8. The relationship between color coordinates (x, y) and ultrasonic time.

(I24), color coordinates (x, y), phosphor efficacy and maintenance (defined as I24/I2). For the sake of clarity, the dependence of 2 h, 24 h brightness and maintenance on the ultrasonic time were illustrated in Fig. 7. Under the same measurement conditions, the brightness of the phosphors with the ultrasonic treatment is higher than that of the commercial ones. The ultrasonic treatment has an evident effect on the brightness of the phosphors. The 2 h brightness of the phosphor amazingly increased by 198% ($42.09 \rightarrow 125.48\ cd/m^2$) after the ultrasonic treatment of 30 min. The two curves for brightness in Fig. 7 have the same trends, that is, the brightness of the phosphors was improved remarkably with the ultrasonic time increases from 0 to 30 min; and then the brightness descends with ultrasonic time further increasing. As mentioned above, there exist defects in the samples with a distorted hexagonal or cubic crystalline form caused by ultrasonic treatment. Furthermore, a longer ultrasonic time led to more defects. After the annealing process at 750 °C, the copper activator might preferentially precipitate on these defects with a concentration exceeding their solubility limit in ZnS host [21,22]. So, in the phosphors the distribution of copper activators is non-uniform. Some regions are rich in copper while other regions are mainly ZnS with relatively perfect lattice. The case is extremely beneficial to the EL performance of the ZnS:Cu,Cl phosphors [21,22]. Consequently, the brightness of the samples increased remarkably with the ultrasonic time increases from 0 to 30 min. However, when the ultrasonic time is further prolonged, the brightness descends. This may be due to that the integrity of the ZnS lattice was overdamaged, and the excess defects trapped electrons or holes, hindering them to radiatively recombine and emit light. Hence, the defects in the microstructure induced by the ultrasonic treatment are the fundamental reason for the change of EL brightness of the phosphors. The maintenances of the phosphors treated by the ultrasound are equal to or better than that of the commercial ones, as shown in Fig. 7. The relationship between color coordinates and the ultrasonic time was displayed in Fig. 8. The x and y values range from 0.184 to 0.188 and from 0.416 to 0.460, respectively. They both increase monotonically with the increase of ultrasonic time, indicating that the color of the light emitted by the phosphors gradually changes from bluish green to green. In addition, it is found from Table 1 that the efficacies of the phosphors ultrasonicated for 15 min (5.97 lm/W) and 30 min (5.68 lm/W) are higher than that of the commercial ones (5.62 lm/W), while the efficacies of the phosphors ultrasonicated for 45, 60 min or without ultrasonic treatment are lower than that of the commercial ones. In summary, the overall performances of the phosphors subjected to ultrasonic treatment for 15 and 30 min are superior to the commercial ones; the phosphors treated by ultrasound for 45 and 60 min have higher performance than commercial ones in 2 and 24 h brightness and maintenance. Therefore, the ZnS:Cu,Cl phosphors prepared by the present method have potential applications for EL devices.

4. Conclusions

The ZnS:Cu,Cl phosphors were prepared by high-temperature (1150 °C) solid-state reaction, subsequent ultrasonic treatment ($t = 0$–60 min) and the final low-temperature annealing process at 750 °C. XRD indicates that ultrasonic treatment benefits the form of ZnS cubic phase which is essential for the efficient EL performances of the ZnS:Cu,Cl phosphors. UV–vis absorbance spectra demonstrate that increase of ultrasonic time results in a slight red-shift of the absorption edge for the phosphors. Ultrasonic treatment exhibits strong influences on the PL and EL properties. Generally, PL performance monotonically declines with a longer ultrasonic time. In contrast, the phosphors treated by ultrasound for 45 and 60 min have higher EL performance than commercial ones in 2 h, 24 h brightness and maintenance. Moreover, the overall performances of the phosphors subjected to ultrasonic treatment for 15 and 30 min are superior to the commercial ones. The defects in the microstructure induced by the ultrasonic treatment are the

fundamental reason for the change of PL and EL performances. The ZnS:Cu,Cl phosphors prepared by the present method have potential applications for EL devices.

Acknowledgment

This research was financially supported by National Science Foundation of China Grant 20471068, Shanghai Pujiang Program Grant 05PJ14101 and Shanghai Fundamental Research Grant 05JC14080.

References

[1] P.D. Rack, P.H. Holloway, Mater. Sci. Eng., R 21 (1998) 171.
[2] X. Wu, D. Carkner, H. Hamada, I. Yoshida, M. Kutsukake, K. Dantani, in: Proceedings of Society for Information Display Conference, May 2004, Seattle, USA, 2004, p. 1146.
[3] Y.A. Ono, Electroluminescent Displays, World Scientific, Singapore, 1995.
[4] K. Manzoor, V. Aditya, S.R. Vadera, N. Kumar, T.R.N. Kutty, Solid State Commun. 135 (2005) 16.
[5] Y. Nien, I. Chen, Appl. Phys. Lett. 89 (2006) 261906.
[6] J.P. Kim, M.R. Davidson, M. Puga-Lambers, E. Lambers, P.H. Holloway, J. Lumin. 109 (2004) 75.
[7] N.E. Brese, C.L. Rohrer, G.S. Rohrer, Solid State Ionics 123 (1999) 19.
[8] S. Sundar Manoharan, Q. Mohammad, Phys. Status Solidi A 202 (2005) 1124.
[9] O. Ehlert, A. Osvet, M. Batentschuk, A. Winnacker, T. Nann, J. Phys. Chem. B 110 (2006) 23175.
[10] S. Kawashima, Jpn. J. Appl. Phys. 5 (1966) 1161.
[11] B. Arterton, J.W. Brightwell, S. Mason, B. Ray, I.V.F. Viney, J. Cryst. Growth 117 (1992) 1008.
[12] H. Chander, V. Shanker, D. Haranath, S. Dudeja, P. Sharma, Mater. Res. Bull. 38 (2003) 279.
[13] S. Han, I. Singh, D. Singh, Y. Lee, G. Sharma, C. Han, J. Lumin. 115 (2005) 97.
[14] L. Armelao, D. Camozzo, S. Gross, E. Tondello, J. Non-Cryst. Solids 345–346 (2004) 402.
[15] K. Manzoor, S.R. Vadera, N. Kumar, T.R.N. Kutty, Appl. Phys. Lett. 84 (2004) 284.
[16] Y. Tang, Y. Jiang, Z. Jia, B. Li, L. Luo, L. Xu, Inorg. Chem. 45 (2006) 10774.
[17] B.J. Fitzpatrick, J. Cryst. Growth 86 (1990) 106.
[18] D.W.G. Ballentyne, J. Electrochem. Soc. 107 (1960) 807.
[19] G. Sharma, S. Han, J. Kim, S.P. Khatkar, Y. Rhee, Mater. Sci. Eng., B 131 (2006) 271.
[20] F. Huang, J.F. Banfield, J. Am. Chem. Soc. 127 (2005) 4523.
[21] A.G. Fischer, J. Electrochem. Soc. 109 (1962) 1043.
[22] A.G. Fischer, J. Electrochem. Soc. 110 (1963) 733.